

Figure 2. NMR spectra of 0.1 mM OL₁ DNA at pH 7.0 in 200 mM KCl, 50 mM potassium phosphate, 1 mM EDTA, 99.9% D₂O. All spectra were taken at 30 °C. (A) The top trace shows the aromatic proton spectrum of OL₁ in the absence of nitrogen-15 decoupling. This spectrum was the average of 2000 transients; each spectrum was accumulated at 2 Hz per point resolution, and a relaxation delay of 2 s followed each transient. The bottom trace shows the difference between spectra taken with and without broad-band ¹⁵N decoupling under the same conditions as for the top trace. This trace shows that G₄, G₃, and G₆ were specifically labeled at N-7 and the protons at C-8 have chemical shifts of 7.55, 7.70, and 7.48 ppm, respectively. (B) These spectra are identical with the bottom spectrum in part A, except that they were acquired with specific-frequency ¹⁵N decoupling. Each experiment was the average of 500 transients. This figure shows that the ¹⁵N chemical shifts for the three guanines are somewhat different; they are approximately 88.8, 88.3, and 88.8 ppm (relative to G N-1 of tRNA) for G₃, G₄, and G₆, respectively.

was appropriately blocked and the phosphoramidite derivative prepared.^{25,26} The phosphoramidite derivative was then used in an Applied Biosystems 381A DNA synthesizer to prepare the 17 base pair OL₁ fragment. The operator fragments were then purified by reverse-phase HPLC according to Stec et al.²⁷ Incorporation of [^{7-¹⁵N}]-2'-deoxyguanosine was carried out only for three marked guanosine residues of strand ii.

Figure 2A shows ¹⁵N difference decoupled spectra of the aromatic region of OL₁. Three major proton peaks can be seen

(23) [^{7-¹⁵N}]Guanine (40 mL; 10 mM) in 1 N HCl was added to 200 mL of 0.2 M Tris and immediately back-titrated to pH 7.0. To this were added 100 mg of 2-deoxyribose 1-phosphate and 1 mg of calf thymus purine nucleoside phosphorylase (twice dialyzed against 0.1 M Tris chloride, pH 7.0; approximately 20 units). The reaction was monitored at 305 nm. When the absorbance decrease ceased (approximately 20 min), the reaction mixture was quickly frozen, lyophilized, and purified over a large Sephadex G-10 column (350 mL) equilibrated with pH 3.5 acetic acid.

(24) Roy, S.; Hiyama, Torchia, D. A.; Cohen, J. S. *J. Am. Chem. Soc.* **1986**, *108*, 1675.

(25) Jones, R. A. In *Oligonucleotide Synthesis; A Practical Approach*; Gait, M., Ed.; IRL Press: Oxford, 1984.

(26) Caruthers, M. H.; Barone, A. D.; Beucage, S. L.; Dodds, D. R.; Fisher, E. F.; McBride, L. J.; Matteucci, M.; Stabinsky, Z.; Tang, J. Y. *Methods Enzymol.* **1987**, *154*, 287.

(27) Stec, W. J.; Zon, G.; Uznanski, B. *J. Chromatogr.* **1985**, *326*, 263.

in the difference spectra at 7.479, 7.545, and 7.695 ppm. They correspond to C-8H protons of guanines 6, 3, and 4, respectively.²⁸ The ¹⁵N-¹H two-bond coupling is 11 Hz. The spectrum of the aromatic region is similar to the reported OL₁ spectrum.²⁸

Figure 2B shows selective ¹⁵N difference decoupled spectra of the OL₁ fragment. The intensities of the three proton peaks are modulated at different nitrogen frequencies as the selective decoupling is stepped through at 25-Hz intervals in the ¹⁵N dimension. We estimate that there is some chemical shift dispersion in the nitrogen dimension.

In conclusion, we have developed a synthetic procedure to label N-7 positions of 2'-deoxyguanosines and incorporated them in a 17 base pair synthetic oligomer. We have shown by selective difference decoupling that the three guanine residues differ somewhat in ¹⁵N chemical shift. The 11-Hz coupling constant with the C-8H proton would allow use of HMQC techniques for nitrogen-15 assignment and indirect detection through C-8H protons. Significant sequence dependence of the ¹⁵N-7 chemical shifts as well as ease of assignment and sensitive detection through protons should make [^{7-¹⁵N}]purine-labeled oligonucleotides valuable for studying protein-nucleic acid interaction.

Supplementary Material Available: Characterization of 4-hydroxy-2,5,6-triaminopyrimidine, [¹⁵N]guanine, and [¹⁵N]-2'-deoxyguanosine (1 page). Ordering information is given on any current masthead page.

(28) Weiss, M.; Patel, D. J.; Sauer, R. T.; Karplus, M. *Proc. Natl. Acad. Sci. U.S.A.* **1984**, *81*, 130.

Synthesis of Novel Polyfunctional Nickel(II)-Nickel(II) Dimer Ni₂Cl₂[C(SiMe₃)(PMe₃)₂]₂ by Photolysis of the First [(Trimethylsilyl)diazomethyl]nickel(II) Complex Ni[C(N₂)SiMe₃]Cl(PMe₃)₂

Herbert König,[†] Marie Joëlle Menu,[‡] Michèle Dartiguenave,^{*‡} Yves Dartiguenave,^{*‡} and H. F. Klein^{*‡}

Laboratoire de Chimie Inorganique
Université P. Sabatier
205 route de Narbonne, F-31077 Toulouse, France
Anorganische Chemie I, E. Zintl Institute
Technische Hochschule, Hochschulstrasse 10
D6100 Darmstadt, Federal Republic of Germany
Received October 11, 1989

A growing number of transition-metal complexes have been reported, in which a diazoalkane is N-coordinated to the metal. Catalytic or photocatalytic elimination of N₂ produces carbenoid intermediates that have been used in synthesis and are thought to be key systems in homogeneous catalysis.¹ Occasionally, introduction of C-bonded diazoalkane functionality into transition-metal complexes has been achieved using LiC(N₂)R or Hg[C(N₂)R]₂ reagents with Os(NO)Cl(PPh₃)₃,² RhCl(PMe₃)₄,³ or PdCl₂(PR₃)₂.⁴

As the first example of a C-bonded 3d metal diazoalkane complex, we report on the synthesis of the Ni(II) compound Ni[C(N₂)SiMe₃]Cl(PMe₃)₂. Photoinduced elimination of N₂ gives rise to a novel Ni-Ni-bonded dinuclear compound containing two phosphorus ylide bridges as analyzed by an X-ray diffraction study.

Treatment of (PMe₃)₂NiCl₂ with 1 equiv of LiC(N₂)SiMe₃ in THF below -25 °C generates Ni[C(N₂)SiMe₃]Cl(PMe₃)₂ (1) in

[†]Anorganische Chemie I, E. Zintl Institute, Technische Hochschule.

[‡]Laboratoire de Chimie Inorganique Université P. Sabatier.

(1) Herrmann, W. A. *Angew. Chem., Int. Ed. Engl.* **1978**, *17*, 800-812.

(2) Gallop, M. A.; Jones, T. C.; Rickard, C. E. F.; Roper, W. R. *J. Chem. Soc., Chem. Commun.* **1984**, 1002.

(3) Menu, M. J.; Desrosiers, P.; Dartiguenave, M.; Dartiguenave, Y.; Bertrand, G. *Organometallics* **1987**, *6*, 1822-1824.

(4) Muharashi, S. I.; Kitani, Y.; Uno, T.; Hosokawa, T.; Miki, T.; Yine-zawa, T.; Kasai, N. *Organometallics* **1986**, *5*, 356-365.

Table I. Crystal Data and Details of Data Collection and Structure Refinement for $[\text{NiCl}(\text{SiMe}_3)(\text{PMe}_3)]_2$

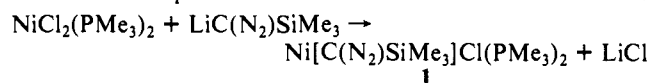
| | |
|--|---|
| formula | $\text{Ni}_2\text{Cl}_2\text{Si}_2\text{P}_2\text{C}_{14}\text{H}_{36}$ |
| cryst system | monoclinic |
| space group | $I2/m$ |
| a , Å | 9.428 (1) |
| b , Å | 11.282 (2) |
| c , Å | 11.272 (2) |
| β | 99.20 (1) |
| V , Å ³ | 1183.5 (6) |
| Z | 8 |
| d_{calcd} , g/cm ³ | 1.434 |
| temp, °C | 20 ± 2 |
| scan method | $\theta/2\theta$ |
| data collectn range (θ), deg | $1 < \theta < 35$ |
| no. of reflectns measured | 3483 |
| no. of unique data with $(I) > 3\sigma(I)$ | 1647 |
| no. of parameters refined | 69 |
| R^a | 0.0481 |
| R_w^b | 0.0527 |

^a $R = \sum ||F_o| - |F_c|| / \sum |F_o|$. ^b $R_w = [\sum w(|F_o| - |F_c|)^2 / \sum w|F_o|^2]^{1/2}$; $w = 1/s^2(|F_o|)$.

Table II. Fractional Atomic Coordinates with Estimated Standard Deviations in Parentheses

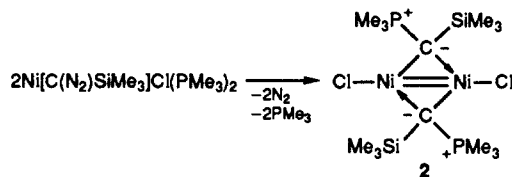
| atom | x/a | y/b | z/c |
|------|------------|------------|------------|
| Ni | 0.5000 (0) | 0.6011 (7) | 0.5000 (0) |
| Cl | 0.5000 (0) | 0.7910 (2) | 0.5000 (0) |
| C1 | 0.4720 (6) | 0.5000 (0) | 0.6297 (5) |
| P | 0.3793 (2) | 0.5000 (0) | 0.2561 (1) |
| Si | 0.7138 (2) | 0.5000 (0) | 0.3315 (2) |
| C11 | 0.2088 (8) | 0.5000 (0) | 0.3053 (7) |
| C12 | 0.3735 (6) | 0.3705 (5) | 0.1611 (5) |
| C13 | 0.3735 (6) | 0.6295 (5) | 0.1611 (5) |
| C21 | 0.7181 (9) | 0.5000 (0) | 0.1648 (6) |
| C22 | 0.8157 (6) | 0.6358 (5) | 0.3890 (5) |
| C23 | 0.8157 (6) | 0.3642 (5) | 0.3890 (5) |

a smooth high-yield reaction.⁵ Air-sensitive dark green crystals of **1** that decompose above -25 °C are obtained from toluene.



In the infrared region, crystals of **1** display an intense $\nu(\text{CN}_2)$ band at 1955 cm⁻¹, characteristic of a C-coordinated diazoalkane. As evidenced by NMR, a trans configuration around the nickel is adopted in solution [NMR at -80 °C, C₇D₈; ³¹P NMR, singlet, -13.07 ppm; ¹H NMR, two singlets, 1.24 ppm (18 H, PMe₃) and 0.54 ppm (9 H, SiMe₃); ¹³C NMR, two singlets, 12.7 ppm (PMe₃) and 0.83 ppm (SiMe₃)].

Photolysis⁶ transforms **1** into a new compound **2**, which is isolated as air-stable green crystals that persist up to 205 °C.



(5) A solution of $\text{Li}(\text{N}_2)\text{SiMe}_3$ (3.2 mmol) freshly prepared from $\text{HC}(\text{N}_2)\text{SiMe}_3$ and BuLi in 10 mL of THF at -80 °C was added to solid $\text{NiCl}_2(\text{PMe}_3)_2$ (0.9 g, 3.2 mmol). The solution was then stirred at -50 °C for 15 min until the color changed to dark green. The temperature was then increased to -25 °C and the solvent removed under vacuum. The residue was extracted with cold toluene. The solution, filtered at -25 °C and concentrated under vacuum, gave rise to small green crystals in nearly quantitative yield. Their decomposition starts at about 10 °C.

(6) A typical experiment: 0.45 g of $\text{Ni}[\text{C}(\text{N}_2)\text{SiMe}_3](\text{PMe}_3)_2$ (1.25 mmol) was dissolved in 25 mL of toluene at -25 °C in an 80-mL quartz ampule, which was then sealed under vacuum. This green solution was irradiated at 300 nm. After 30 min it turned red. At this point, it was transferred to a flask, concentrated, and cooled to -30 °C for 15 h. Dark green crystals were precipitated. These were washed with ether and dried in vacuo, giving 0.27 g of $[\text{Ni}_2\text{Cl}_2\{\text{C}(\text{SiMe}_3)(\text{PMe}_3)\}_2]$ (84% yield). Anal.: Found (calcd) for $\text{C}_{14}\text{H}_{36}\text{Cl}_2\text{Ni}_2\text{P}_2\text{Si}_2$ (510.88): C, 32.70 (32.91); H, 7.20 (7.10).

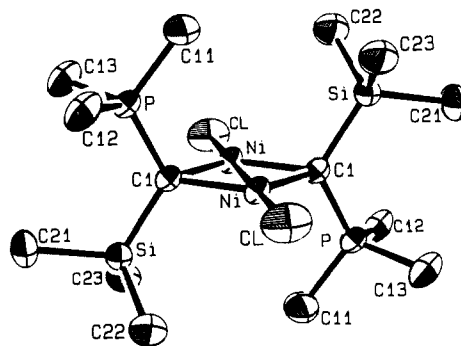


Figure 1. Crystal structure of **2** (ORTEP, thermal ellipsoids 50%, without H atoms) (distances in angstroms; angles in degrees): Ni-Ni, 2.281 (1); Ni-Cl, 2.143 (2); Ni-C1, 1.906 (4); C1-P, 1.746 (6); P-C11, 1.783 (8); P-C12, 1.807 (6); P-C13, 1.807 (6); C1-Si, 1.872 (6); Si-C21, 1.885 (7); Si-C22, 1.868 (6); Si-C23, 1.868 (6); Ni-Ni-C1, 180.1 (6); Ni-C1-Ni, 73.5 (2); C1-Ni-C1, 106.5 (1); Cl-Ni-C1, 126.8 (1); Ni-C1-P, 111.9 (2); Ni-C1-Si, 115.5 (2); P-C1-Si, 120.0 (4).

In view of the very simple ³¹P and ¹H NMR spectra of the dimeric molecule **2** ($m/e = 508$, ⁵⁸Ni, ³⁵Cl) [¹H NMR, doublet at 1.93 ppm (²J_{PH} = 13 Hz; 18 H, PMe₃), singlet at 0.38 ppm (18 H, SiMe₃); ³¹P NMR, singlet at 30 ppm] that are not conclusive and the observation of ¹³C signals for all but two bridging carbon nuclei, a single-crystal X-ray diffraction of **2** was undertaken.⁷

The structure (Figure 1) reveals the presence of two symmetrically bridging three-electron-donor ylide ligands. The central ring Ni₂Cl₂ is planar, and the two chlorine atoms belong to this plane. The Si, P, C21, C11, and C1 atoms are also coplanar, this plane being perpendicular to the Ni₂Cl₂ ring. The distribution of the angles, with Ni-C1-Ni = 73.5 (2)° and C1-Ni-C1 = 106.5 (1)°, strongly supports the presence of a Ni-Ni bonding interaction. Since the compound is formally a Ni(II) derivative, two electrons are available on each nickel and therefore a double bond is expected. In agreement with this is the Ni-Ni distance of 2.281 (1) Å, which is the shortest distance reported for binuclear Ni complexes.⁸ The Ni-C1 distance in the ring [1.906 (4) Å] is slightly shorter than the usual values of Ni(II)-sp³ C bonds and may indicate an sp² C atom, in agreement with the P-C1-Si angle of 120.0 (4)°. The C1-P1 distance, 1.746 (6) Å, is shorter than the three distances P-C11, P-C12, and P-C13 [average 1.780 (8) Å] in PMe₃ and is in the range expected for phosphorus ylides bridging two metal centers [1.750 (1)–1.82 (4) Å]. Most notable is the pronounced shortening of the Ni-Cl distance [2.143 (2) Å] which must be a consequence of the tight bonding situation of the nickel atoms. The rotational positions of the PMe₃ and SiMe₃ groups are in a staggered conformation with respect to each other, in line with the overall centrosymmetry of the molecule.

Generation of the dinuclear complex **2** by loss of dinitrogen implies the formation of a carbyne nickel moiety, which is expected to be unstable. Subsequently a carbyne bridge could be formed that is finally stabilized by addition of phosphine to give the observed ylide bridges. There are precedents for the phosphine addition to carbyne tungsten carbonyl systems.⁹ Reaction of other

(7) Crystal structure data: monoclinic, space group $I2/m$; $a = 9.428$ (1) Å; $b = 11.282$ (2) Å; $c = 11.272$ (2) Å; $\beta = 99.20$ (1)°; $Z = 8$; 1647 independent diffraction data [$I \geq 3\sigma(I)$]; $R = 0.0481$, $R_w = 0.0527$. Measurement: Enraf-Nonius CAD4 (Mo K α). Resolution: SHELX 76.

(8) Some examples of Ni-Ni distances. Ni(0): Einspahr, H.; Donohue, J. *Inorg. Chem.* **1974**, *13*, 1839–1843; DeLaet, D. L.; Fanwick, P. E.; Kubiak, C. P. *Organometallics* **1986**, *5*, 1807–1811. DeLaet, D. L.; del Rosario, R.; Fanwick, P. E.; Kubiak, C. P. *J. Am. Chem. Soc.* **1987**, *109*, 754–758. Osborn, J. A.; Stanley, G. G.; Bird, P. H. *J. Am. Chem. Soc.* **1988**, *110*, 2117–2122. DeLaet, D. L.; Powell, D. R.; Kubiak, C. P. *Organometallics* **1985**, *4*, 954–957. Ni(I): Mills, O. S.; Shaw, B. W. *J. Organomet. Chem.* **1968**, *11*, 595–600. Adams, R. D.; Cotton, F. A.; Rusholme, G. A. *J. Coord. Chem.* **1971**, *1*, 275–283. Kruger, C. *Angew. Chem., Int. Ed. Engl.* **1969**, *8*, 678. Jones, R. A.; Stuart, A. L.; Atwood, J. L.; Hunter, W. E.; Rogers, R. D. *Organometallics* **1982**, *1*, 1721–1723. Ni(II): Melson, G. A.; Greene, P. T.; Bryan, R. F. *Inorg. Chem.* **1970**, *9*, 1116–1122.

nucleophiles together with the potential use of this functionalized Ni–Ni dimer in synthesis is under active investigation.

Acknowledgment. We thank the Ministre des Affaires Étrangères (France) and the DAAD (Germany) for their support through the PROCOPE program and a DAAD fellowship to H.K.

Supplementary Material Available: Tables of bond lengths, bond angles, atomic coordinates, and thermal parameters for **2** (2 pages); listing of observed and calculated structure factors for **2** (8 pages). Ordering information is given on any current masthead page.

(9) Kreissl, F. R.; Friedrich, P.; Lindner, T. L.; Huttner, G. *Angew. Chem., Int. Ed. Engl.* **1977**, *16*, 314. Jeffery, J. C.; Navarro, R.; Razay, H.; Stone, F. G. A. *J. Chem. Soc., Dalton Trans.* **1981**, 2471–2478.

Temperature-Independent Long-Range Electron Transfer Reactions in the Marcus Inverted Region

Nong Liang,[†] John R. Miller,^{*†} and Gerhard L. Closs^{*†,‡}

Chemistry Division, Argonne National Laboratory
Argonne, Illinois 60439
Department of Chemistry, The University of Chicago
Chicago, Illinois 60637

Received February 26, 1990

The Marcus theory made the remarkable prediction that rates of highly exoergic electron transfer (ET) reactions would slow down with increasing thermodynamic driving force ($-\Delta G^\circ$) and give rise to a so-called inverted region.¹ Although that prediction was controversial for two decades,² a number of groups have now confirmed the bell-shaped free-energy dependence of rates on ΔG° .³ According to the Marcus theory in its original, classical form, the inverted region is caused by the reappearance of an activation energy when the negative free energy is larger than λ , the reorganization energy. We report here the measurements of the temperature dependence of two highly exoergic intramolecular ET reactions providing a direct critical test of this theory. Although these reactions have previously been shown to fall deep into the inverted region, they show almost no activation energies in accord with theories that include quantum-mechanical treat-

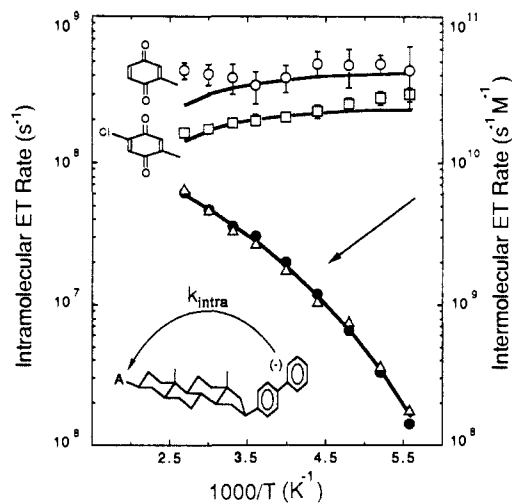


Figure 1. Temperature dependence of intramolecular (upper) and intermolecular (lower) electron transfer rate constants. The solid line at the lower portion represents the best fit to the VTF equation (see text for detail; open triangle, CIQSB; solid circle, QSB). The solid lines at the upper portion were calculated by eq 1 with the experimentally determined parameters from refs 3d and 6. For clarity, the theoretical $k_{\text{intra}}(T)$ of CIQSB has been multiplied by a factor of 1.69. At this stage, we tend to attribute the minor discrepancies between the theory and the experiment to the oversimplification of our model. Three independent experiments at concentrations of 30, 9.6, and 7.3 mM, respectively, were performed for QSB, while for CIQSB, two experiments (23 and 11 mM) were performed.

ments of high-frequency molecular vibrations of the donor and acceptor groups.⁴

The reactions studied were the intramolecular charge shift ETs from the negative ion of a 4-biphenyl group (B^-), attached to the 16-position of 5 α -androsterone (S), to a 2-benzoquinonyl (Q, $\Delta G^\circ = -2.10$ eV), QSB, or 5-chloro-2-benzoquinonyl (CIQ, $\Delta G^\circ = -2.29$ eV), CIQSB, at the 3-position of the steroid (inset, Figure 1). The ions were generated in 2-methyltetrahydrofuran (MTHF) by pulse radiolysis, reaction rates were measured by fast transient absorption spectroscopy, and the data were analyzed as described previously.^{3d,h} The temperature range of the measurements reached from -94 to 100 °C. In another set of experiments, intermolecular rates were measured between the monofunctional steroids B⁻S and QS or CIQS. By subtraction of the intermolecular rates from the total ET rates obtained on the bifunctional compounds, the intramolecular rate constants were obtained.^{3h}

In Figure 1, k_{intra} and k_{inter} are plotted against $1/T$. Clearly k_{intra} for both QSB and CIQSB is almost temperature independent, with slower rates for the more exoergic CIQSB. This observation cannot be explained by the classical Marcus theory, which predicts a change of k_{intra} of more than 3 orders of magnitude over the temperature range studied.⁵ On the other hand, eq 1 provides an excellent description (solid lines in upper Figure 1) using parameters that were determined independently and were published earlier.^{3d}

(4) (a) Levich, V. G.; Dogonadze, R. R. *Dokl. Akad. Nauk SSSR* **1960**, *133*, 158. (b) Kestner, N. R.; Logan, J.; Jortner, J. *J. Phys. Chem.* **1974**, *78*, 2148. (c) Van Duyne, R. P.; Fischer, S. F. *Chem. Phys.* **1974**, *5*, 183. (d) Ulstrup, J.; Jortner, J. *J. Chem. Phys.* **1975**, *63*, 4358. (e) Efrima, S.; Bixon, M. *Chem. Phys.* **1976**, *13*, 447. (f) Fischer, S. F.; Van Duyne, R. P. *Chem. Phys.* **1977**, *26*, 9. (g) Siders, P.; Marcus, R. A. *J. Am. Chem. Soc.* **1981**, *103*, 741. (h) Siders, P.; Marcus, R. A. *J. Am. Chem. Soc.* **1981**, *103*, 748. (i) Marcus, R. A. *J. Chem. Phys.* **1984**, *81*, 4494. Excellent reviews: (j) Ulstrup, J. *Charge Transfer Processes in Condensed Media*; Springer-Verlag: Berlin, 1979. (k) Devault, D. *Quantum Mechanical Tunneling in Biological Systems*, 2nd ed.; Cambridge Univ. Press: Cambridge, 1984. (l) Newton, M. D.; Sutin, N. *Annu. Rev. Phys. Chem.* **1984**, *35*, 437. (m) Marcus, R. A.; Sutin, N. *Biochim. Biophys. Acta* **1985**, *811*, 265.

(5) The estimate was made in the contemporary classical formulation (Sutin, N.; Brunshwig, B. S.; Creutz, C.; Winkler, J. R. *Pure Appl. Chem.* **1988**, *60*, 1817): $k = 2|V|^2(\pi^3/\lambda h^2 k_B T)^{1/2} \exp[-(\lambda + \Delta G^\circ)^2/4\lambda k_B T]$; $\lambda = \lambda_a + \lambda_b$. From 100 to -94 °C, k_{intra} would decrease by factors of 200 for QSB and 3000 for CIQSB.

[†] Argonne National Laboratory.

[‡] The University of Chicago.

(1) Marcus, R. A. *Discuss. Faraday Soc.* **1960**, *29*, 21.

(2) (a) Rehm, D.; Weller, A. *Isr. J. Chem.* **1970**, *8*, 259. (b) Bock, C. R.; Meyer, T. J.; Whitten, D. G. *J. Am. Chem. Soc.* **1975**, *97*, 2909. (c) Frank, A.; Gratzel, M.; Henglein, A.; Janata, E. *Ber. Bunsen-Ges. Phys. Chem.* **1976**, *80*, 547. (d) Creutz, C.; Sutin, N. *J. Am. Chem. Soc.* **1977**, *99*, 241. (e) Jonah, C. D.; Metheson, M. S.; Meisel, D. *J. Am. Chem. Soc.* **1978**, *100*, 449. (f) Nagle, J. K.; Dresick, W. J.; Meyer, T. J. *J. Am. Chem. Soc.* **1979**, *101*, 3993. (g) Wallace, W. L.; Bard, A. J. *J. Phys. Chem.* **1979**, *83*, 1350. (3) (a) Beitz, J. V.; Miller, J. R. *J. Chem. Phys.* **1979**, *71*, 4579. (b) Calcaterra, L. T.; Closs, G. L.; Miller, J. R. *J. Am. Chem. Soc.* **1983**, *105*, 670. (c) Miller, J. R.; Beitz, J. V.; Huddleston, R. K. *J. Am. Chem. Soc.* **1984**, *106*, 5057. (d) Miller, J. R.; Calcaterra, L. T.; Closs, G. L. *J. Am. Chem. Soc.* **1984**, *106*, 3047. (e) McLendon, G.; Miller, J. R. *J. Am. Chem. Soc.* **1985**, *107*, 7811. (f) Wasielewski, M. R.; Niemczyk, M. P.; Svec, W. A.; Pewitt, E. B. *J. Am. Chem. Soc.* **1985**, *107*, 1080. (g) Irvine, M. B.; Harrison, R. J.; Beddard, G. S.; Leighton, P.; Sanders, J. K. M. *Chem. Phys.* **1986**, *104*, 315. (h) Closs, G. L.; Calcaterra, L. T.; Green, N. J.; Penfield, K. W.; Miller, J. R. *J. Phys. Chem.* **1986**, *90*, 3673. (i) Harrison, R. J.; Pearce, B.; Beddard, G. S.; Cowan, J. A.; Sanders, J. K. M. *Chem. Phys.* **1987**, *116*, 429. (j) Gould, I. R.; Ege, D.; Mattes, S. L.; Farid, S. *J. Am. Chem. Soc.* **1987**, *109*, 3794. (k) Ohno, T.; Yoshimura, A.; Shioyama, H.; Mataga, N. *J. Phys. Chem.* **1987**, *91*, 4365. (l) Closs, G. L.; Miller, J. R. *Science* **1988**, *240*, 440. (m) Gould, I. R.; Moody, R.; Farid, S. *J. Am. Chem. Soc.* **1988**, *110*, 7242. (n) Gould, I. R.; Farid, S. *J. Am. Chem. Soc.* **1988**, *110*, 7883. (o) Mataga, N.; Kanda, Y.; Asahi, T.; Miyasaka, H.; Okada, T.; Kakitani, T. *Chem. Phys.* **1988**, *127*, 239. (p) Mataga, N.; Asahi, T.; Kanda, Y.; Okada, T.; Kakitani, T. *Chem. Phys.* **1988**, *127*, 249. (q) Asahi, T.; Mataga, N. *J. Phys. Chem.* **1989**, *93*, 6575. (r) Chen, P.; Duesing, R.; Tapolsky, G.; Meyer, T. J. *J. Am. Chem. Soc.* **1989**, *111*, 3993. (s) Gould, I. R.; Moser, J. E.; Armitage, B.; Farid, S.; Goodman, J. L.; Herman, M. S. *J. Am. Chem. Soc.* **1989**, *111*, 1917. (t) Meade, T. J.; Gray, H. B.; Winkler, J. R. *J. Am. Chem. Soc.* **1989**, *111*, 4353.